Theoretical investigation of chemical and morphological ordering in Pd_cCu_{1-c} clusters

C. Mottet and G. Tréglia
CRMC2—CNRS, Campus de Luminy, Case 913, F-13288 Marseille Cedex 9, France*

B. Legrand
SRMP-DMN, CEA Saclay, F-91191 Gif-sur-Yvette Cedex, France

(Received 20 November 2001; revised manuscript received 1 March 2002; published 25 July 2002)

We present a theoretical study of Pd_cCu_{1-c} clusters from a few hundred to a few thousand of atoms, using Monte Carlo simulations and quenched molecular dynamics. This is performed within tight-binding many-body potentials, the tight-binding Ising model and the second moment approximation, which properly account for chemical and structural changes at transition-metal surfaces. The respective stabilities of the fcc, bcc, and icosahedral cluster shape are discussed in terms of competition or synergy between surface segregation and bulk ordering. Besides a finite-size effect on surface segregation, due to the limited quantity of matter, we show that chemical ordering can induce some geometrical frustrations and enhance the stability of ''stoichiometric'' clusters, the composition of which is strongly size dependent. Finally, it is found that chemical ordering leads to morphological transitions at equiconcentration.

DOI: 10.1103/PhysRevB.66.045413 PACS number(s): 61.46.+w, 61.66.Dk, 64.60.Cn, 82.60.Qr

I. INTRODUCTION

Bimetallic clusters are widely used in the field of heterogeneous catalysis. Indeed they present both a size effect, consisting in an enhancement of the reactivity when the particles size decreases,[1] and an alloying effect illustrated by the concentration dependence of the selectivity.[2] As an example, a strong size effect has been evidenced in the case of Pd-supported clusters for CO chemisorption[3] and catalytic hydrogenation of 1,3-butadiene.[4] On the other hand, it has been shown that alloying Pd particles with Cu extends the temperature range in which one can maintain a high turnover rate for CO oxidation,[5] and also greatly enhances its selectivity in the partial hydrogenation of dienes.[6]

The understanding of the reaction mechanisms proceeds through the accurate determination of both the atomic structure and morphology of the clusters, and of the chemical ordering and surface segregation phenomena that they undergo. Even though they can be modified by the reaction,[7] their knowledge before the reaction is a useful guide for a more general understanding.

From an experimental point of view, a major problem when studying such systems comes from the difficulty to obtain collections of particles with an homogeneous distribution in size, morphology, and, for bimetallic compounds, chemical composition, in order to perform unambiguous analysis.[8] Such a goal has been reached in the case of PdCu clusters supported on relatively inert substrates, prepared either by condensation of the two metals under ultrahigh vacuum[9,10] or from organometallic precursors.[11–13] Indeed, the analysis of these clusters by x-ray diffraction,[11,13] electron microscopy,[10,12] or high-resolution electron microscopy[9,12] shows that, except in one study,[13] they are perfectly ordered with the B2 CsCl structure when the thermodynamical equilibrium is achieved. In addition, surface segregation of Cu has been observed, and confirmed by numerical simulations performed on fcc-type polyhedra.[11,13]

Anyway, before modeling supported bimetallic clusters, a first step is to model free ones, with the aim to predict at least the local chemical arrangement for a given morphology. In what concerns the morphology of free clusters made of pure fcc elements, both theoretical[14–19] and experimental[20] studies agree on the existence of a morphological transition from icosahedral (Ih) to truncated octahedral (TO) fcc structure when the size increases. One can then wonder about the morphology adopted by bimetallic clusters, and also to what extent their size and morphology will influence surface segregation and chemical ordering phenomena.

Therefore, we study here the coupling between the chemical arrangement and the geometrical structure for free Pd_cCu_{1-c} clusters of different sizes. We used Monte Carlo simulations and quenched molecular-dynamics simulations within energetic models derived from a tight-binding description of the electronic structure, by combining the tight-binding Ising model (TBIM) and the second moment approximation (SMA) that have given rise to a large amount of theoretical studies on alloys surfaces (see Ref. 21 for a review).

The paper is organized as follows. In Sec. II the energetic models (TBIM and SMA potentials) are briefly described together with the relaxation algorithms (molecular dynamics, Monte Carlo). Section III is devoted to the influence of the size effect on the segregation isotherms in Pd_cCu_{1-c} unrelaxed fcc clusters. Then we show in Sec. IV the influence of the relaxation of the atomic structure on the chemical arrangement, with some particular emphasis on the icosahedron (fivefold symmetry) and dodecahedron (Dh) that is a bcc-type polyhedron.

II. THEORETICAL MODEL

A. Energetic models

Many aspects of ordering phenomena in alloys have been described using an effective tight-binding Ising model obtained by developing the energy in a perturbative form with respect to the energy of the disordered state on a rigid

lattice.[22] Such a model has been extended to the surfaces of alloys, referred to as the TBIM.[23] It describes in a realistic way surface segregation and ordering phenomena at bimetallic surfaces.[24–26]

However, to study the coupling between structural and chemical arrangements in the peculiar case of clusters, one has to be able to go beyond the rigid lattice assumption of the TBIM in order to perform atomic relaxations in the same time as the optimization of the chemical configuration. Therefore, one needs an interatomic potential depending on the interatomic distances which allows both to displace and to exchange atoms of different species. This is the case of the many-body potentials derived within the SMA of the tight-binding model,[27] which have been widely used for surface and cluster studies, first in pure metals,[28–30,18,19] and then in alloys.[31,32] However, it is necessary to emphasize that such models are, in principle, not sufficient to account properly for ordering effects. Actually the hopping integrals, as treated in SMA, introduce only nondiagonal disorder, whereas most ordering effects in transition alloys have been explained by including essentially diagonal disorder effects, assuming the hopping integrals to be independent of the nature of the atoms in the TBIM scheme.[33] A consistent treatment of both chemical and structural effects requires to go beyond the second moment model. Nevertheless, we choose here to use the SMA potentials but that a parametrization that takes into account the main results of the TBIM, as discussed in the following.

1. The tight-binding Ising model

When only chemical order in an A_cB_{1-c} alloy is studied on a rigid lattice, the tight-binding formalism allows us to derive some effective pair interactions describing chemical ordering and segregation effects near a surface. In this model, the (small) part of the total energy of the system, which involves the chemical configuration dependence, obeys the following Hamiltonian:

$$H^{eff}=\sum_n p_n\left(\Delta h_n^{eff}-\sum_{m\neq n} V_{nm}\right)+\sum_{n,m\neq n} p_n p_m V_{nm}, \quad (1)$$

where

(i) p_n is the occupation number equal to 1 or 0 depending on that the site n is occupied or not by an atom of type A (for a binary alloy A_cB_{1-c}, $p_n=0$ means that the site n is occupied by an atom of type B).

(ii) The local field Δh_n^{eff} is the difference in excess energies at site n between the pure constituents A and B. It vanishes as soon as a site recovers its full bulk coordination. For a surface site, it is identical to the difference in surface energies ($\Delta h_{surf}{}^{eff}=\gamma^A-\gamma^B$).

(iii) The (alloy) effective pair interaction between atoms at sites n and m :

$$V_{nm}=\frac{1}{2}(V_{nm}^{AA}+V_{nm}^{BB}-2V_{nm}^{AB}) \quad (2)$$

is generally negligible for fcc alloys beyond nearest neighbors. Its sign for a pair of first neighbors characterizes the tendency to bulk ordering ($V>0$) or to phase separation ($V<0$).

Because of the rigid lattice assumption made in the TBIM, such model does not treat the possible atomic relaxations induced by the size mismatch between the two components. Moreover, in the particular case of clusters that present some bulk symmetry deviations together with important atomic structure relaxations, we need to go beyond the TBIM assumption in order to treat reasonably the geometrical effects.

2. The second moment approximation model

Within SMA (Ref. 27) the band energy of an atom of type i located at site n is proportional to the square root of the second moment of the local density of states, leading to the many-body character of the potential. This band energy term writes

$$E_{n,b}^i(\{p_m^j\})=-\sqrt{\sum_{\substack{m\\ r_{nm}<r_c}}\sum_{j=A,B} p_m^j \xi_{ij}^2 e^{-2q_{ij}[(r_{nm}/r_{ij})^o-1]}}, \quad (3)$$

and is counterbalanced by a repulsive term of the Born-Mayer type,

$$E_{n,r}^i(\{p_m^j\})=\sum_{\substack{m\\ r_{nm}<r_c}}\sum_{j=A,B} p_m^j A_{ij} e^{-p_{ij}[(r_{nm}/r_{ij}^o)-1]}, \quad (4)$$

where r_{nm} is the distance between the atoms at sites n and m, $r_{ii}^o, i=A,B$, is the nearest-neighbor distance in the pure metal i, $r_{ij}^o=(r_{ii}^o+r_{jj}^o)/2$ if $i\neq j$, and r_c is the cutoff distance for the interactions. $\{p_m^j\}$ represents the chemical configuration of the system, in which p_m^j is the occupation number defined before. The parameters $(A_{ij},p_{ij},q_{ij},\xi_{ij})$ are fitted to different experimental values.

The total energy of the system is then written as follows :

$$E_{tot}(\{p_n^i\})=\sum_n\sum_{i=A,B} p_n^i[E_n^{i,b}(\{p_m^j\})+E_n^{i,r}(\{p_m^j\})]. \quad (5)$$

This analytical expression can then be used in two different ways depending on the problem addressed. For atomic relaxations, it allows us to get interatomic forces, which can then be used in quenched molecular-dynamics simulations to determine the equilibrium atomic positions of the system at $T=0$ K.[31] For chemical equilibrium studies at finite temperatures, Monte Carlo simulations are used by calculating energy balances involved during exchanges.

3. Parametrization of the TBIM versus the SMA

SMA parametrization. Usually, the homoatomic interactions in the SMA potential are fitted to bulk properties: cohesive energy E_{coh}, lattice parameter (a),[34] and elastic constants (B,C_{44},C') (Ref. 35) of the pure metals. In the present study, we choose to fit the parameters $(A_{ii},p_{ii},q_{ii},\xi_{ii})$ to the surface energies (γ_{surf}) (Ref. 36) and

TABLE I. Parameters values for Pd and Cu. The experimental values are noted in parentheses: Lattice parameter a and cohesive energy are taken from Ref. 34, elastic constants (B, C_{44}, C') from Ref. 35 and surface energies (γ_{surf}) from Ref. 36.

	A (eV)	p	ξ (eV)	q	a (nm)	B (GPa)	C_{44} (GPa)	C' (GPa)	γ_{surf} (eV/atom)	E_{coh} (eV/atom)
Pd	0.358	7.352	3.722	2.384	0.389	196	84	23	0.965	−8.936
					(0.389)	(195)	(71)	(29)	(0.95)	(−3.89)
Cu	0.115	9.184	1.802	1.880	0.361	140	86	25	0.730	−5.17
					(0.361)	(142)	(82)	(26)	(0.73)	(−3.49)

not to the cohesive ones in order to follow one of the main driving forces of surface segregation deduced from the TBIM.[23] A first major consequence of this choice is to prevent a Pd surface segregation in the whole range of concentration, as obtained previously by embedded-atom method (EAM),[37] which is inconsistent with experimental observations![11] The corresponding values for Pd and Cu are given in Table I. As can be seen in this table, fitting the parameters to reproduce the surface energies leads to overestimated values of the cohesive energies. This is not surprising since it is well known that such potentials are not satisfactorily transferable from isolated atoms to bulk via surface. This is not only the case in the SMA framework,[27] but also within similar methods such as the EAM (Ref. 38) or the corrected effective medium theory CEM,[39] or with potentials going beyond the second moment within the tight-binding formalism.[40] More precisely, if one fits the value of the cohesive energy, one obtains underestimated values of the surface energy. Nevertheless, these deviations do not prevent to describe correctly the relaxations and/or reconstruction of the low-index surfaces.[28] Even though some empirical attempts have been proposed to reconcile bulk and surface energies, such as the ''bond order metal simulator-mixing model''[41,42] or the ''modified SMA,''[11,43] they are not suited to perform atomic relaxations. In fact, only the *ab initio* methods reproduce reasonably both cohesive and surface energies of transition metals,[44,45] but they are limited to very small sizes.

For the heteroatomic interactions, the parameters are determined in order to account for the main thermodynamical characteristics of the bulk PdCu alloy phase diagram, in particular the ordered phases present at low temperature. From this point of view, a main feature is the existence of a $B2$ ordered phase on a bcc lattice at equiconcentration and not the $L1_0$ one on the fcc lattice.[46] Remember that both Pd and Cu are fcc metals. To take into account this specificity, we have imposed the parameters to fit not only the dissolution energy of Pd in Cu [E_{Cu}(Pd)] but also the formation energy of the $B2$ ordered phase (E_{B2})[46] and its lattice parameter.[47] Moreover, we have constrained the $L1_0$ ordered phase energy (E_{L1_0}) to be higher than the $B2$ one, in order to stabilize the latter with respect to the former, according to the phase diagram.[49] The so-fitted values of the parameters (A,p,ξ,q) for the Pd-Cu interactions are given in Table II, together with the calculated and experimental values of E_{Cu}(Pd), E_{B2}, and a_{B2} used for the fit. We notice that our best fit is not able to reproduce exactly the different energies. The quantity E_{L1_2} (for Cu_3Pd) has been calculated independently and compared with the experimental value. *Ab initio* calculations[48] have been performed using the full potential linear muffin-tin orbitals method in order to give some relevant references when the experimental ones do not exist, notably concerning the $L1_0$ phase.

TBIM parametrization. In the TBIM, the effective pair interaction V is usually fitted to the mixing enthalpy i.e., the formation energy of a disordered alloy phase. For an equiatomic fcc alloy (A_1 phase), this leads to

$$\Delta H_m = -c(1-c)ZV^{fcc} = -3V^{fcc},$$

so that V^{fcc} would be equal to 0.037 eV/atom.[46] Unfortunately, such a value is not sufficient to account for the formation energy of the $B2$ ordered phase at equiatomic concentration. A full consistency with the parametrization of the SMA model then requires to favor the ordering energies : $E_{L1_0} - E_{A1} = -V^{fcc}$ on fcc lattice and $E_{B2} - E_{B1} = -2V^{bcc}$ on bcc lattice, rather than the mixing one. Indeed, reproducing the corresponding energies calculated within the previously described SMA potential (and using a mean-field approximation to evaluate the energies of the disordered phases) lead to much higher values of V: $V^{fcc} = 0.17$ eV/atom ($L1_0$) and $V^{bcc} = 0.19$ eV/atom ($B2$). It is

TABLE II. Parameters values for Pd-Cu interactions. Experimental energy values are taken from Ref. 46 and lattice parameter from Ref. 47; *ab initio* calculations are taken from Ref. 48.

Pd-Cu	A (eV)	p	ξ (eV)	q	$E_{Cu}(Pd)$ (eV/atom)	E_{B2} (eV/atom)	E_{L1_0} (eV/atom)	E_{L1_2} (eV/atom)	a_{B2} (nm)	a_{L1_0} (nm)
	0.208	7.200	2.600	2.867	−0.637	−0.052	−0.049	−0.120	0.296	0.362
Experimental					−0.534	−0.150		−0.105	0.296	
Ab initio						−0.095	−0.079		0.293	0.370

quite nice to find almost the same value in spite of the differences between the two lattice structures, which seems to confirm that pair interactions are essentially governed by interatomic distance.[49]

In the framework of the mean-field approximation, the critical temperatures are given at equiatomic concentration, by $T_c=2V/k$ on fcc lattice and $T_c=4V/k$ on bcc lattice, which are overestimated with respect to ''exact'' calculations by factors of 2.22 and 1.27, respectively.[50] Therefore, $T_c(L1_0)$ should be equal to 1766 K for the transition from the $L1_0$ ordered phase to the $A1$ disordered one on fcc lattice and $T_c(B2)$ should be equal to 6930 K for the transition from $B2$ ordered phase to the $B1$ disordered one on bcc lattice. We have checked that we recover these values via Monte Carlo simulations. If, in a first approximation, we consider entropic effects quite similar for the different phases, it seems reasonable to find $T_c(L1_0)$ smaller than $T_c(B2)$. The only available experimental critical temperature value concerns the transition from the ordered $B2$ phase to the fcc disordered one $A1$, which appears at much lower temperature : $T_c(B2)=850$ K. It has to be noticed that fitting on mixing energy as mentioned before would have given a critical temperature of $T_c=390$ K, which is much lower than the present one. These considerations point out the difficulty to model the order-disorder transition involving structural modifications (changing from fcc to bcc lattice) within the TBIM. In order to derive qualitative trends only, we will study cases well above and well below $T_c(L1_0)=1766$ K, namely, we will determine the segregation isotherms at 0.06 T_c and 2.5 T_c.

B. Relaxation algorithms

Before describing our results, let us recall that our relaxed atomic configurations are nothing but the more stable ones at 0 K (derived from *quenched* molecular dynamics[51]), whereas the Monte Carlo simulations are performed at finite temperatures, without rearrangement of this atomic structure during the chemical equilibrium.

Our aim here is to describe as best as possible the coupling between chemical and structural changes in bimetallic clusters as a function of size, concentration, and temperature. This is a wide problem that can be addressed following different procedures.

A first alternative would be to use a coupled Monte Carlo simulation, in which both displacements and chemical exchanges are proposed at each step, in an attempt to reach the global minimum by exploring the whole subspace of different structural and chemical conformations for each cluster. Unfortunately such an optimization procedure, although it properly accounts for the coupling between chemistry and morphology on a given lattice, is still unable to reveal complete morphological transition from one structure to another (for instance fcc to bcc) induced by chemical rearrangements, at least for large sizes. Indeed such transitions involve collective atomic rearrangements that are out of the scope of the Monte Carlo scheme. To our knowledge, such a global optimization has only been performed on small and pure clusters.[52]

For large enough sizes, where clusters must display the bulk crystalline structure (thousands of atoms), the most suitable theoretical approach is to compare the energies of stable sequences for each various competitive structure[14–19] and to keep the one with the minimum energy. This has the advantage to allow us to characterize metastable states that could become stable under peculiar conditions, and also to be sure having reached the best minimum. For each sequence, surface segregation can be studied by coupling in a self-consistent way molecular dynamics and Monte Carlo simulation by relaxing the atomic positions between two exchanges of unlike atoms. However, to our knowledge, the single study performed in this way for bimetallic clusters[13,53] has been limited to the fcc structure (TO of 201 and 1289 atoms) showing that, when atomic relaxations are small, they do not affect significantly chemical ordering. Therefore, a simpler method is to relax the atomic structure only once, using quenched molecular dynamics at $T=0$ K, and then to determine the equilibrium chemical configuration using Monte Carlo simulation on this relaxed lattice. Then one has just to check that a new relaxation would not change the profile. This is the procedure chosen here, being aware that our study is not complete, but thinking that it can be considered as a preliminary attempt to illustrate the influence of the atomic structure on the chemical ordering and *vice versa*.

The Monte Carlo simulations have been performed in the framework of the Metropolis algorithm.[54] It consists in proposing exchanges between any atom A with any atom B on a rigid lattice. This exchange is accepted or not depends on the energy difference between the two configurations before and after the exchange: if it is negative, it is kept, and if not, it can still be accepted according to a Boltzmann probability $e^{-\Delta E/kT}$. As previously mentioned, the associated energetic balance is calculated within TBIM or SMA potentials. More precisely, the SMA potential is used whenever one deals with Ih bimetallic clusters, whereas the TBIM one is sufficient for the fcc-type clusters. It is worth pointing out that, thanks to the consistency in parametrizing the two potentials, we have checked that both TBIM–Monte Carlo and SMA–Monte Carlo simulations give quantitatively the same results on fcc-type clusters concerning segregation and ordering phenomena.

III. SURFACE SEGREGATION IN FCC TRUNCATED OCTAHEDRA

In this section, we describe the segregation isotherms of Pd_cCu_{1-c} TO of 201 and 1289 atoms using Monte Carlo simulations within the TBIM model. These segregation isotherms represent the variation of the mean Pd concentrations c_X for some given types of sites denoted X, as a function of the global concentration of Pd in the cluster c. X can be used to describe either ''mean'' (surface, volume) or more detailed (edges, facets, core, etc.) geometrically inequivalent sublattices. The corresponding Pd concentration is given by

$$c_X=\frac{1}{N_X}\sum_{i=1}^{N_X} p_i^{Pd}, \tag{6}$$

TABLE III. Numbers of sites of vertex, edge, (100), and (111) facets for the 201- and 1289-atom TO fcc clusters.

Atoms	Vertex	Edge	(100) facet	(111) facet
201	24	36	6	56
1289	24	108	54	296

where N_X is the number of sites of X type given in Table III. The segregation isotherms have been calculated for the cluster mean surface (on Fig. 1) and also for vertex, edge, and (100) and (111) facet sites (on Fig. 2) for the two cluster sizes (201 and 1289 atoms), either in the ordered (at $0.06\,T_c$) or in the disordered state ($2.5\,T_c$), i.e., for two temperatures well below and well above the order-disorder temperature T_c.

A. Disordered state ($T > T_c$): Finite matter effect

At high temperature ($T = 2.5T_c$), the segregation isotherms [see Figs. 1(b,d)] show a weak segregation of Cu, which is reversed when the clusters are rich in Pd (beyond 70% of Pd). This result is consistent with those obtained by a TBIM study on perfect surfaces of different orientations[55–57] at high temperatures.

The comparison between size of the clusters made of 201 atoms or 1289 atoms shows that surface segregation is quite the same in both cases but the core concentration displays a significant deviation from the global concentration especially in the small cluster. Cu surface segregation in both cases takes Cu atoms from the core to put them at the surface. When the size decreases, the available quantity of Cu atoms in the cluster becomes more and more limited so that the core concentration is drastically modified by surface segregation, whereas in infinite systems such as flat surfaces, the bulk concentration is unaffected. The finite size effect drives to a *finite matter effect* concerning the segregation phenomenon.

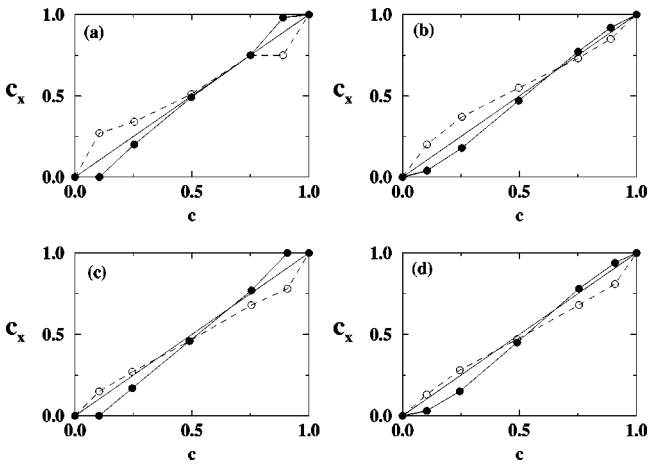

FIG. 1. TBIM segregation isotherms concerning surface (●) and core (○) Pd concentrations of 201-atom (a,b) and 1289-atom (c,d) TO clusters as a function of the global concentration c in Pd at $0.06T_c$ (a,c) and $2.5T_c$ (b,d). The diagonal line represents the absence of segregation.

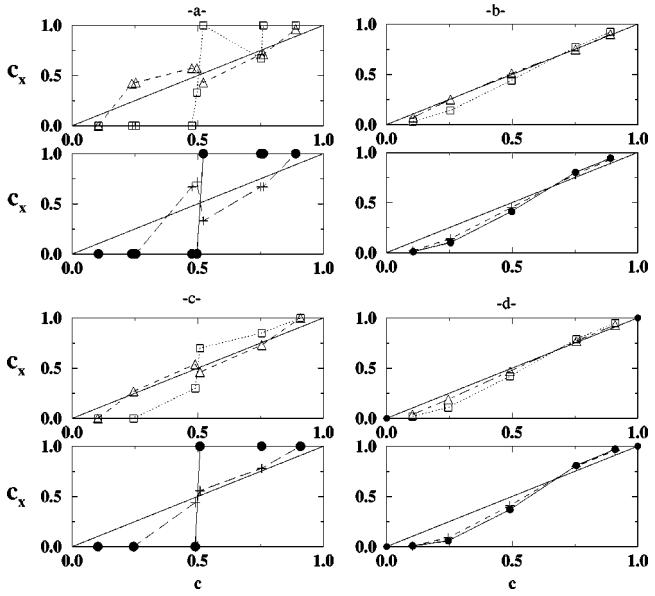

FIG. 2. The same as Fig. 1 for (100) facets (□), (111) facets (△), vertices (●), and edges (+).

Such a phenomenon has been evidenced for small particles of $Ni_{1\,at\%}Pd$ supported by alumina substrate with average sizes in the range 30–100 nm. The strong dependence of equilibrium surface composition with respect to particle size has been analyzed in terms of a ''mass balance model,''[58] which is nothing but the application of the matter conservation rule, involving matter redistribution from the core to the surface of the cluster. However, although such a model indeed accounted qualitatively for the effect of the particle size on surface composition, some discrepancies remained compared to the experimental results. This was tentivatively attributed to ordering phenomena that, as will be seen in the following for Pd_cCu_{1-c} TO, can indeed play a major role.

B. Ordered state ($T < T_c$): Finite-size geometrical frustration

At low temperature ($T = 0.06T_c$), the surface segregation isotherms [see Fig. 1(a,c)] are not so different from those at high temperature. However, if we decompose the surface of the clusters into coordination-type sites (vertices, edges, and facets, as done in Fig. 2), the corresponding segregation isotherms are very inhomogeneous showing some local order effects that disappear at high temperature. The general rule of increasing segregation when the site coordination is decreasing is obeyed (at least at high temperature) even if it is not very pronounced. At low temperatures, sharp transitions are observed between Cu-poor and Cu-rich site compositions, for types of sites involving only a small number of atoms. This is the case for vertices (24 atoms), but also (for small sizes) for the (100) facets sites of the 201-atom size (only six atoms).

A more detailed analysis of the way the clusters try to account for chemical ordering as a function of their size and morphology shows the existence of geometrical frustrations, induced by the simultaneous occurrence of facets with various orientations, that have to intersect with one another.

Before analyzing in detail the case of clusters, it is worth reminding the simple cases of the (111) and (100) faces of single crystals for which there already exists either a compe-

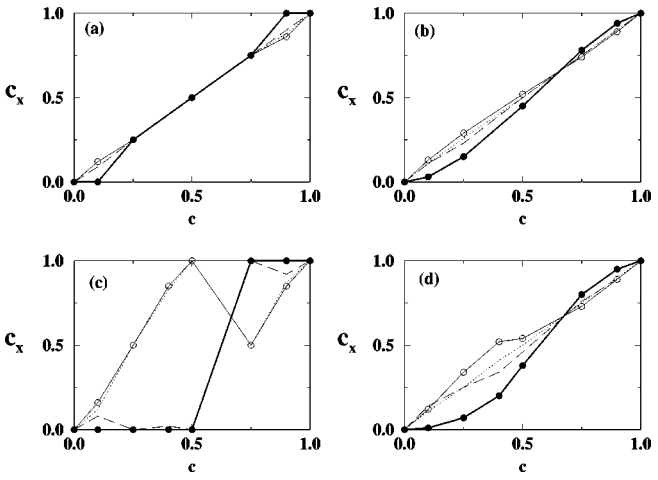

FIG. 3. TBIM segregation isotherms concerning (111) (a,b) and (100) (c,d) Pd_cCu_{1-c} perfect surfaces at $0.06T_c$ (a,c) and $2.5T_c$ (b,d); the 1st, 2nd, 3rd, and 4th planes starting from the surface are represented respectively by (●),(○), dashed line, and dotted line.

tition or a synergy (depending on the concentration) between surface segregation and bulk ordering (see Refs. 55–57 for theoretical results and Ref. 59 for experimental confirmation). We have illustrated the main results on surface segregation isotherms on the Fig. 3 using the present model, but it is better referring to Refs. 55–57 for a complete and detailed study. We see in Fig. 3 for the two surfaces a segregation reversal from Cu-rich system where Cu segregates to Pd-rich system where Pd segregates. This is mainly due to the alloying effect that leads to the segregation of the majority element whereas surface energy criterion favors Cu segregation for any bulk concentration. Moreover, Fig. 3 shows that the two orientations display an oscillating profile at $T>T_c$, corresponding to alternate Cu and Pd enrichments, as expected from the tendency to chemical ordering of the system. The segregation is larger in the (100) surface than in the (111) one. At $T<T_c$, the oscillations are stronger at the (100) surface and disappear at the (111) surface. For the (111) orientation, the segregation isotherm displays some concentration range with constant segregation or no segregation (around $c=0.4$).[56] In the (100) case, we find an alternate stacking of either pure layers at $c=0.5$, or pure and mixed ones for $c=0.25$ or $c=0.75$, which are Cu terminated or Pd terminated depending on concentration since the segregation is reversed after the equiconcentration.

Note that, at equiconcentration, there exists another variant for the (100) surface, made of a stack of mixed planes, but which is found less stable than the first one (see a similar study on Cu_cPt_{1-c}.[60]) This variant will be referred to as ''mixed'' with respect to the previous ''alternate'' one.

Clusters are specific systems that present simultaneously facets with different crystallographic orientations [(111) and (100) facets] and where the two (alternate and mixed) variants present in the (100) staking can coexist in the ordered state. This is illustrated in Fig. 4(a) [or also in Fig. 5(a)], where we see clearly the geometrical truncations of the fcc cluster in the $L1_0$ ordered phase driving to two Cu-pure (100) facets and four mixed (100) facets. We checked that the (100) facet concentration in Fig. 2 is indeed the average value between the two variants. As the alternate variant (Cu-pure/Pd-pure) is the most favorable from an energetical point of view as mentioned above, we could have expected to get only this one for all the (100) facets of the cluster. This is not the case because the cluster prefers to keep a perfect core ordering following the $L1_0$ phase. This illustrates the *geometrical frustration* of surface segregation and ordering phenomena in bimetallic clusters. This result contradicts the conclusions of a previous study performed on PdCu clusters, in terms of a face-dependent surface segregation and a layer-alternating atomic concentration profile.[13] Such geometrical frustration does not exist for example in the bcc cluster ordered according to the $B2$ phase as illustrated in Fig. 4(b), where all the facets are mixed.

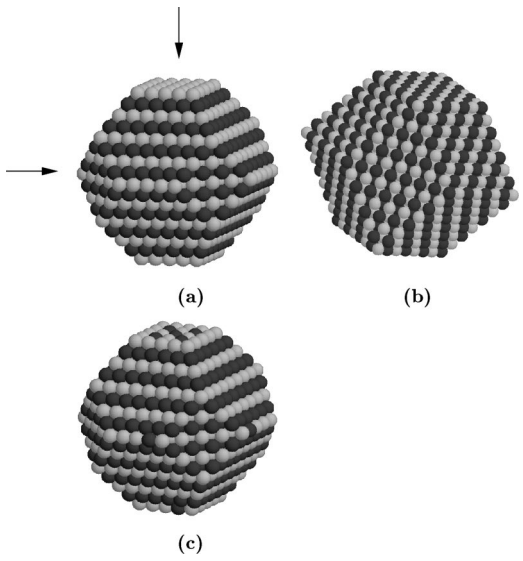

FIG. 4. Snapshots of ordered 1289-atom TO (dark sphere are Pd atoms and clear ones are Cu ones): the $Cu_{657}Pd_{632}$ fragment of the $L1_0$ bulk phase (a) and $Cu_{645}Pd_{644}$ (c), and ordered B2 bcc dodecahedron $Cu_{848}Pd_{847}$ (b).

C. Ordered state ($T<T_c$): Size-dependent stoichiometry

Let us first recall a main result of the theoretical studies devoted to surface segregation in ordered alloy.[21] At suffi-

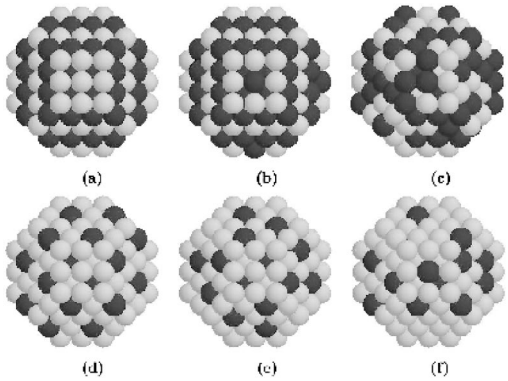

FIG. 5. Snapshots of the 201-atom TO (dark sphere are Pd atoms and clear ones are Cu ones): the $Cu_{105}Pd_{96}$ fragment of the $L1_0$ bulk phase (a), $Cu_{101}Pd_{100}$ at $0.06T_c$ (b), and at $2.5T_c$ (c); then the $Cu_{153}Pd_{48}$ fragment of the $L1_2$ bulk phase (d), $Cu_{150}Pd_{51}$ at $0.06T_c$ (e), and at $2.5T_c$ (f).

TABLE IV. Size-dependent perfect stoechiometry for the 201- and 1289-atom Cu_NPd_M TO fcc clusters near equiatomic concentration.

Atoms	c	N	M
201	0.48	105	96
1289	0.49	657	632

ciently low temperature, the more stable surface termination is the ideal one, i.e., the one that corresponds to the perfect ordered stacking. This result implies, for a finite system, that the concentrations that allow a perfect chemical ordering to be achieved in the whole cluster should correspond to an enhanced stability. Indeed slight variations from these concentrations (off-stoichiometry), will induce antisite defects that will cost some energy and then decrease stability. This is illustrated by the snapshots of Figs. 5(a) and 5(b) for the 201-atom clusters and in the snapshots of Figs. 4(a) and 4(c) for the 1289-atom clusters. The fragments of the bulk $L1_0$ ordered phases with the TO morphology driving to clusters Cu_NPd_M with concentration slightly different from 0.5 where N and M, noted in Table IV, correspond to an ideal stoichiometry compared to the one obtained at $c=0.5$, i.e., $N \sim M$. TO fcc clusters with $N \sim M$ [(Figs. 5(b) and 4(c)] present some antisite defects compared to the perfect ordered one [Figs. 5(a) and 4(a)]. Any size is not compatible with any concentration for getting the best ordered structure, so that ''stoichiometric clusters'' have to be introduced to describe chemical order effect related to chemical composition, in addition to the ''magic numbers'' related to an enhanced stability for given cluster sizes.

Looking at the clusters at composition about 0.25, we notice that surface segregation modifies the ''perfectly ordered $L1_2$'' cluster in Figs. 5(d) and 5(e) for $c=0.25$, since the minority atoms prefer to be inside the cluster in order to maximize the number of heteroatomic bonds.

Now, from a more general point of view, we can regret that simulations on such systems have been limited generally to the TO disordered clusters shown in Figs. 5(c) and 5(f),[11,41,42,53] apart for some ''pioneering'' works on rigid icosahedral and cuboctahedral bimetallicclusters with up to 147 atoms.[37] Indeed, it is well known that small monometallic fcc clusters adopt compact shapes, such as the Ih one that minimizes the surface energy.[14–20] Moreover, in the case of the PdCu system, even the bulk fcc phase competes with the bcc one since, at equiconcentration and low temperature, the alloy orders along $B2$ phase on a bcc lattice. It is then difficult to reduce the study of the respective stabilities of Pd-Cu clusters to a chemical rearrangement on an fcc-type morphology.

We study in the following section the case of the relaxed icosahedron structure and the bcc dodecahedral structure.

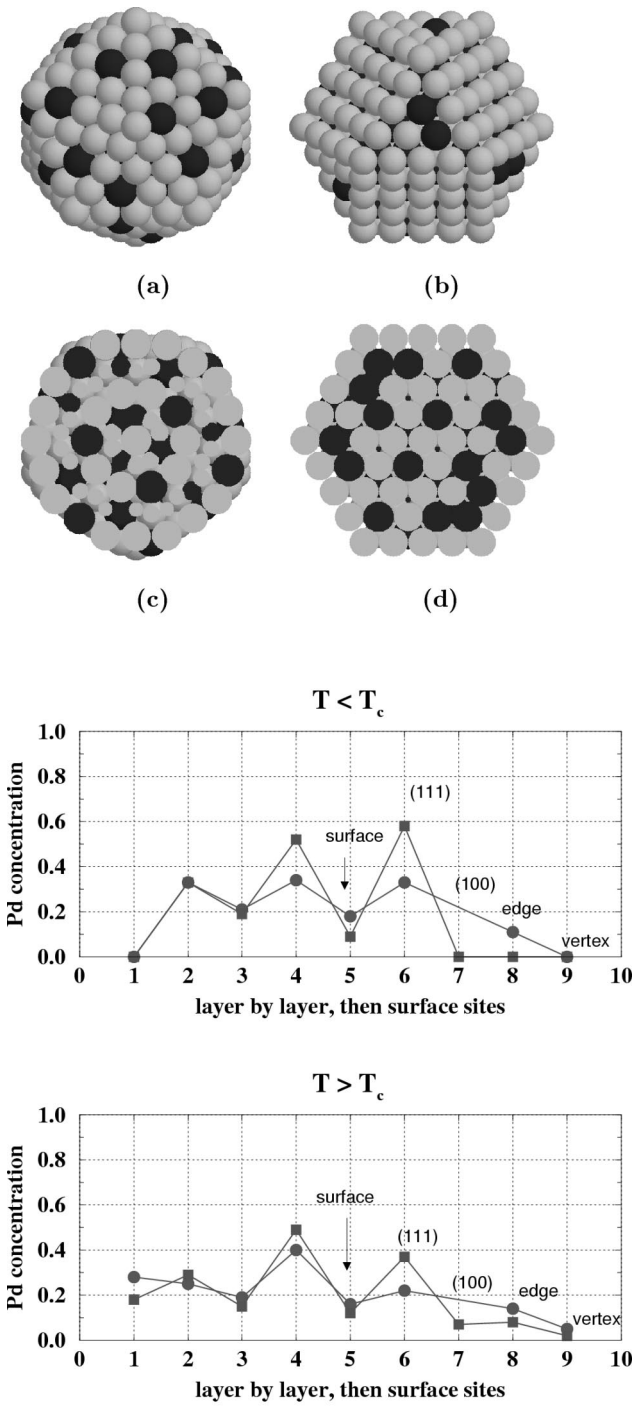

FIG. 6. Snapshots of $Pd_{74}Cu_{235}$ clusters at $0.06T_c$ (dark spheres are Pd atoms and clear spheres are Cu atoms) in the SMA model: relaxed Ih (a) and cuboctahedron (b); (c,d) are respectively the same as (a,b) but with a cross section; the two graphs (at $0.06T_c$ and at $2.5T_c$) illustrate the concentration profiles of the two types of cluster (● for the relaxed Ih and □ for the cuboctahedron) by concentric layers going from the center to the surface and for the different kind of sites at the surface.

IV. INTER-RELATION BETWEEN CHEMICAL ORDER AND THE MORPHOLOGICAL SHAPE

A. The icosahedral morphology

As mentioned above, the fcc structure is not always the stablest one for clusters made of pure fcc metals[14–20] and some experiments have related the existence of stable Au-Fe alloy icosahedral nanoparticles.[61] It is well known that small pure clusters prefer the icosahedral shape with the fivefold symmetry in order to minimize the surface energy by form-

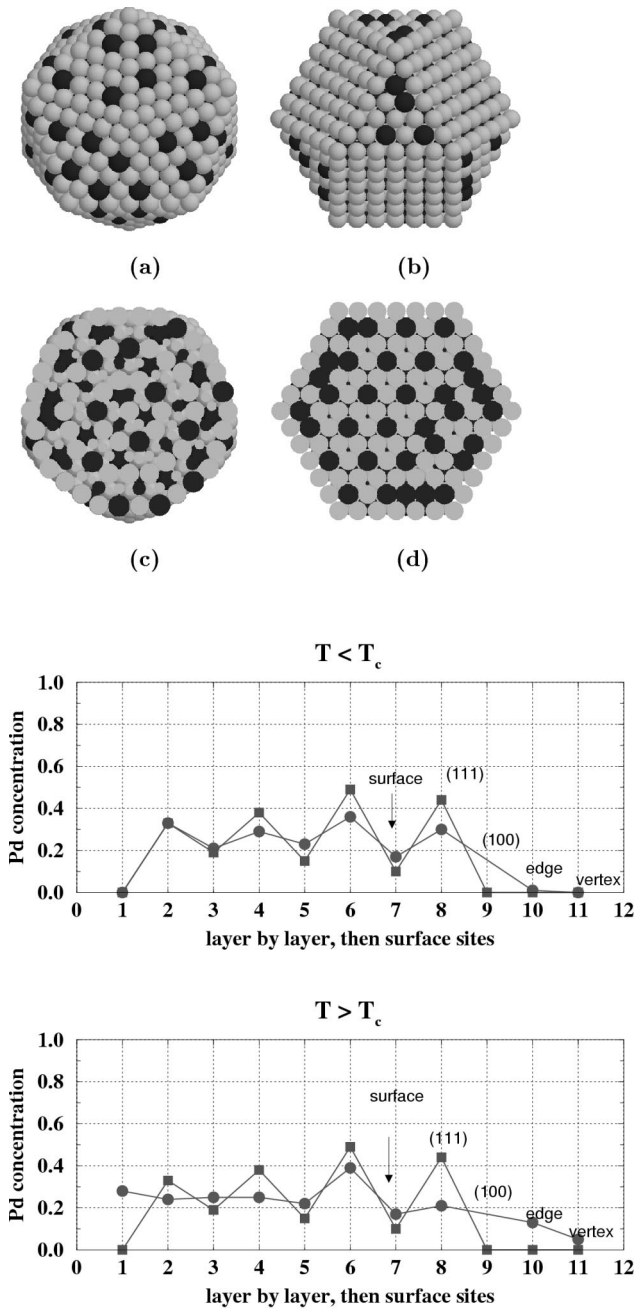

FIG. 7. The same as Fig. 6 for $Pd_{230}Cu_{693}$.

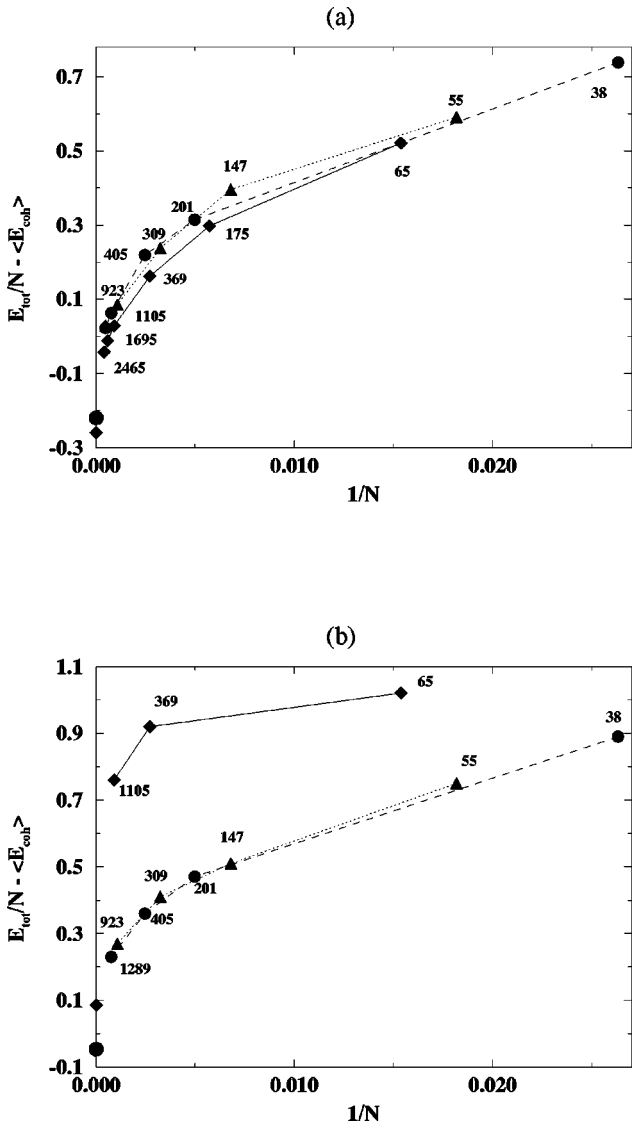

FIG. 8. Relative stabilities of $Cu_{0.5}Pd_{0.5}$ clusters of different morphologies: Dh ($\diamond$), Ih ($\triangle$), and TO ($\bullet$) versus their sizes at $0.06T_c$ (a) and $2.5T_c$ (b); the values at the origin ($1/N=0$) characterize the bulk phases values: at $0.06T_c$ the values correspond to the formation energy of the two ordered phases $L1_0$ and $B2$.

ing only pseudo (111) facets at the surface.[62] But the Ih core, which no longer keeps the fcc symmetry, is constrained. As a consequence, the Ih undergoes an inhomogeneous contraction both at its surface and in its center.[18] We will illustrate here the influence of atomic structure, i.e., fivefold symmetry compared to fcc one, on chemical ordering by performing Monte Carlo simulations within the SMA potential on relaxed Mackay icosahedron[63] and fcc structure in the cuboctahedral shape for a given concentration ($c=0.25$).

Before describing our results, let us recall that our relaxed atomic configurations are nothing but the more stable ones at 0 K (derived from quenched molecular dynamics), whereas the Monte Carlo simulations are performed at finite temperatures, without rearrangement of this atomic structure during the chemical equilibrium. This means (as previously explained) that we treat only partially the coupling between the chemical and the structural arrangements. However, this is justified here since we have checked that we recover sensibly the same concentration profiles for unrelaxed and relaxed fcc clusters.

Snapshots of Figs. 6 and 7 for both 309-atom and 923-atoms clusters, show that Cu atoms are quite homogeneously distributed in the cluster both in the core and at the surface. In the fcc case, the cluster core adopts the $L1_2$ bulk ordering, (as in the previously studied TO), but this ordering is perturbed close to the surface because of geometrical frustrations. If we look at the curve that gives the Pd concentration per atomic shell (Figs. 6 and 7), we notice that they are quite similar for the relaxed icosahedron and cuboctahedron, at least in the core of the clusters. They present a slight Pd

enrichment just under the surface and a Cu segregation at the surface. It is more difficult to compare the two surfaces since they do not involve similar sites. Nevertheless, we observe that Pd atoms occupy preferably the (111) facet sites (with the higher coordination numbers). At any temperature, the cuboctahedron follows an oscillating profile, whereas for the Ih it only occurs at low temperature, losing any order reminding in the disordered state ($T > T_c$). Therefore, ordering at low temperature does not depend so much on the atomic structure (for the relaxed icosahedra and the cuboctahedra), but ordering tendency is lost at high temperature in the icosahedral structure. As a conclusion, this preliminary study shows that, at $c = 0.25$, atomic relaxations on the Ih leads to a ''pseudo ordering'' at low temperature, which is quite comparable to the $L1_2$ ordering in the cuboctahedron, in spite of the fivefold symmetry. The next step in the future should be obviously to improve the coupling between chemistry and atomic relaxations in order to explore the whole concentration range.

B. The dodecahedral morphology

Let us conclude our study by the equiatomic case, where we must consider an other morphology: the dodecahedral (Dh) on bcc lattice. Indeed, knowing that $Pd_{0.5}Cu_{0.5}$ bulk alloy forms a bcc ordered phase ($B2$), one can wonder whether the small particles of such an alloy adopt the same symmetry as the one in the bulk, or if they prefer to crystallize within the competing Ih structure.

The recent experimental observations by HRTEM of $Pd_{0.5}Cu_{0.5}$ (Refs. 10–12) clusters deposited on a MgO(100) substrate have shown that these clusters adopt the $B2$ ordered phase under equilibrium conditions. More precisely, the ordered $B2$ particles exhibit both (110) and (100) faces. Unfortunately, up to now, no experimental study has been performed on free $Pd_{0.5}Cu_{0.5}$ clusters that could give information on their morphology.

From the theoretical point of view, we will then complete our study by adding the Dh shape to the previous fcc-type structures. This morphology is illustrated on Fig. 4(b) and consists in 12 (110) close-packed faces. One can notice that the absence of chemical frustration of $B2$ ordering on this lattice prevents the formation of antisite defects, as it was the case in the fcc structure. We have compared (Fig. 8) the relative stability of the $Pd_{0.5}Cu_{0.5}$ clusters following the three different morphologies in a large range of sizes by comparing the mean energies per atoms: $E_{tot}/N - \langle E_{coh} \rangle$ where $\langle E_{coh} \rangle$ is defined as $\langle E_{coh} \rangle = (N_{Cu}/N_{tot}) E_{coh}^{Cu} + (N_{Pd}/N_{tot}) E_{coh}^{Pd}$.

In the ordered state [$T < T_c$, Fig. 8(a)] the Dh is the most stable structure at any size whereas this morphology is strongly unfavorable in the disordered state [$T > T_c$, Fig. 8(b)]. The chemical $B2$ ordering reverses the structural stability found for pure metallic clusters. This is an evidence of a chemical driven morphological transition.

V. CONCLUSIONS

The present theoretical study of free Pd_cCu_{1-c} clusters shows that the respective stabilities of the different cluster shapes, such as fcc and bcc polyhedra and fivefold Ih, are driven by the competition or synergy between surface segregation and core ordering. In particular, we show finite-size effects on chemical configuration due to the limited quantity of matter. We show how fcc TO clusters in the $L1_0$ phase can lead to geometrical/chemical frustrations at equiatomic concentration with the coexistence of alternate and mixed variant, whereas bcc clusters in the $B2$ phase presents only mixed facets. As a consequence, at equiatomic concentration, chemical ordering can lead to morphological transitions from fcc or fivefold compact structures to more open but chemically nonfrustrated bcc ones. Finally we show the existence of size-dependent stoichiometries related to chemical concentration preventing antisite defects. Such ''stoichiometric'' clusters present an enhanced stability (by analogy with magic numbers related to optimized morphology) and could drive to peculiar properties in catalysis. We show also that the composition at specific surface sites (edges or vertex) can change drastically (from 0% to almost 100% in Pd) with a small variation of overall composition. If a catalytic step can occur only at these specific surface sites, the overall activity of a catalyst could presumably change as abruptly as the concentration of the active metal at these surface sites.

*The CRMC2 is also associated with the Universities of Aix-Marseille II and III.

[1] M. Che and C.O. Bennett, Adv. Catal. **36**, 55 (1989).

[2] J. H. Sinfelt, *Bimetallic Catalysts* (Wiley, New York, 1983); T.E. Hoost, G.W. Graham, M. Shelef, O. Alexeev, and B.C. Gates, Catal. Lett. **38**, 57 (1996); G. Diaz, A. Gómez-Cortés, and M. Benaissa, *ibid.* **38**, 63 (1996); C.P. Vinod, K.R. Harikumar, G.U. Kulkarni, and C.N.R. Rao, Top. Catal. **11**, 293 (2000).

[3] C.R. Henry, C. Chapon, C. Goyhenex, and R. Monot, Surf. Sci. **272**, 283 (1992).

[4] B. Tardy, C. Noupa, C. Leclercq, J.C. Bertolini, A. Hoareau, M. Treilleux, J.P. Faure, and G. Nihoul, J. Catal. **129**, 1 (1991).

[5] K.I. Choi and M.A. Vannice, J. Catal. **131**, 36 (1991).

[6] J. Philips, A. Auroux, G. Bergeret, J. Massardier, and A. Renouprez, J. Phys. Chem. **97**, 3565 (1993).

[7] D. Bazin, C. Mottet, and G. Tréglia, Appl. Catal., A **200**, 47 (2000).

[8] C.R. Henry, Surf. Sci. Rep. **31**, 231 (1998).

[9] P.L. Gai and B.C. Smith, Ultramicroscopy **34**, 17 (1990).

[10] F. Gimenez, C. Chapon, S. Giorgio, and C.R. Henry, Electron Microscopy **2A**, 351 (1994).

[11] A. J. Renouprez, K. Lebas, G. Bergeret, J. L. Rousset, and P. Delichère, in *Studies in Surface Science and Catalysis*, edited by J. W. Hightower, W. N. Delgass, and A. T. Bell (Elsevier Science B.V., 1996), Vol. 101, p. 1105.

[12] S. Giorgio, C. Chapon, and C.R. Henry, Langmuir **13**, 2279 (1997); S. Giorgio and C.R. Henry, Microsc. Microanal. Microstruct. **8**, 379 (1997).

[13] L. Zhu, K.S. Liang, B. Zhang, J.S. Bradley, and A.E. DePristo, J. Catal. **167**, 412 (1997).

[14] C.L. Cleveland and U. Landman, J. Chem. Phys. **94**, 7376 (1991).
[15] S. Valkealahti and M. Manninen, Phys. Rev. B **45**, 9459 (1992).
[16] J. Uppenbrink and D.J. Wales, J. Chem. Phys. **96**, 8520 (1992).
[17] G. D'Agostino, A. Pinto, and S. Mobilio, Phys. Rev. B **48**, 14 447 (1993).
[18] C. Mottet, G. Tréglia, and B. Legrand, Surf. Sci. Lett. **383**, L719 (1997).
[19] F. Baletto, R. Ferrando, A. Fortunelli, F. Montalenti, and C. Mottet, J. Chem. Phys. **116**, 3856 (2002).
[20] B.D. Hall, M. Flüeli, R. Monot, and J.P. Borel, Phys. Rev. B **43**, 3906 (1991); D. Reinhard, P. Berthoud, D. Ugarte, B. Hall, and R. Monot, Phys. Low-Dim. Struct. **1**, 59 (1994); D. Reinhard, B.D. Hall, P. Berthoud, S. Valkealahti, and R. Monot, Phys. Rev. Lett. **79**, 1459 (1997); D. Reinhard, B.D. Hall, D. Ugarte, and R. Monot, Phys. Rev. B **55**, 7868 (1997).
[21] G. Tréglia, B. Legrand, F. Ducastelle, A. Saúl, C. Gallis, I. Meunier, C. Mottet, and A. Senhaji, Comput. Mater. Sci. **15**, 196 (1999).
[22] F. Ducastelle and F. Gauthier, J. Phys. F: Met. Phys. **6**, 2039 (1976).
[23] G. Tréglia, B. Legrand, and F. Ducastelle, Europhys. Lett. **7**, 575 (1988).
[24] B. Legrand and G. Tréglia, Surf. Sci. **236**, 398 (1990).
[25] G. Tréglia, B. Legrand, J. Eugène, B. Aufray, and F. Cabané, Phys. Rev. B **44**, 5842 (1991).
[26] A. Senhaji, G. Tréglia, and B. Legrand, Surf. Sci. **307**, 440 (1994).
[27] V. Rosato, M. Guillopé, and B. Legrand, Philos. Mag. A **59**, 321 (1989).
[28] M. Guillopé and B. Legrand, Surf. Sci. **215**, 577 (1989).
[29] R. Ferrando and G. Tréglia, Surf. Sci. **331**, 920 (1995).
[30] A. Khoutami, B. Legrand, C. Mottet, and G. Tréglia, Surf. Sci. **307**, 735 (1994).
[31] C. Mottet, G. Tréglia, and B. Legrand, Phys. Rev. B **46**, 16 018 (1992).
[32] A. Khoutami, Thesis, University Paris XI, Orsay, 1993.
[33] F. Ducastelle, in *Order and Phase Stability in Alloys*, edited by F. R. De Boer and D. G. Pettifor, Cohesion and Structure, Vol. 3 (North-Holland, Amsterdam, 1991).
[34] C. Kittel, *Introduction to Solid State Physics*, 7th ed. (Wiley, New York, 1996).
[35] G. Simmons and H. Wang, *Single Crystal Elastic Constants and Calculated Aggregated Properties* (MIT, Cambridge, 1971).
[36] F.R. De Boer, R. Boom, W. C. N. Mattens, A. R. Miedema, and A. K. Nielssen, *Cohesion and Structure* (North-Holland, Amsterdam, 1988).
[37] J.M. Montejano-Carrizales and J.L. Moran-Lopez, Surf. Sci. **239**, 169 (1990); J.M. Montejano-Carrizales, M.P. Iniguez, and J.A. Alonso, Phys. Rev. B **49**, 16 649 (1994).
[38] S. M Foiles, M.I. Baskes, and M.D. Daw, Phys. Rev. B **33**, 7983 (1986).
[39] M.S. Stave, D.E. Sanders, T.J. Raeker, and A.E. DePristo, J. Chem. Phys. **93**, 4413 (1990).
[40] J. Guevara, A.M. Llois, and M. Weissmann, Phys. Rev. B **52**, 11 509 (1995).
[41] L. Zhu and A.E. DePristo, J. Chem. Phys. **102**, 5342 (1995).
[42] L. Zhu and A.E. DePristo, J. Catal. **167**, 400 (1997).
[43] J.L. Rousset, A.M. Cadrot, F. Cadete Santos Aires, A. Renouprez, P. Melinon, A. Perez, M. Pellarin, J.L. Vialle, and M. Broyer, J. Chem. Phys. **102**, 8574 (1995).
[44] M. Methfessel, D. Henning, and M. Scheffler, Phys. Rev. B **46**, 4816 (1992).
[45] H.L. Skriver and N.M. Rosengaard, Phys. Rev. B **46**, 7157 (1992).
[46] R. Hultgren, P. D. Desai, D. T. Hawkins, M. Gleiser, and K. K. Kelley, *Values of the Thermodynamic Properties of Binary Alloys* (American Society for Metals, Berkley, Metals Park, Jossey-Bass Publishers, San Francisco, 1981).
[47] W. B. Pearson, *Handbook of Lattice Spacings and Structures of Metals and Alloys* (Pergamon Press, Oxford, 1964).
[48] A. Saúl (private communication).
[49] F. Ducastelle, J. Phys. (Paris) **31**, 1055 (1970); P. Turchi, Thesis, University Paris VI, 1984.
[50] D. De Fontaine, Solid State Phys. **34**, 174 (1979).
[51] L. Verlet, Phys. Rev. **159**, 98 (1967).
[52] D.J. Wales and J.P.K. Doye, J. Phys. Chem. **101**, 5111 (1997).
[53] L. Yang, T.J. Raeker, and A.E. DePristo, Surf. Sci. **290**, 195 (1993); L. Yang and A.E. DePristo, J. Catal. **148**, 575 (1994).
[54] N. Metropolis, A.W. Metropolis, N.M. Rosenbluth, A.H. Teller and E. Teller, J. Chem. Phys. **21**, 1087 (1953).
[55] C. Gallis, B. Legrand, A. Saúl, G. Tréglia, P. Hecquet, and B. Salanon, Surf. Sci. **352-354**, 588 (1996).
[56] C. Gallis, B. Legrand, and G. Tréglia, Surf. Rev. Lett. **4**, 1119 (1997).
[57] C. Gallis, Thesis, University Paris VI, 1997.
[58] D.O. Groomes and P. Wynblatt, Surf. Sci. **160**, 475 (1985).
[59] A. Rochefort, M. Abon, P. Délichère, and J.C. Bertolini, Surf. Sci. **294**, 43 (1993).
[60] A. Senhaji, Thesis, University Paris XI, Orsay, 1994.
[61] D.K. Saha, K. Koga, and H. Takeo, Eur. Phys. J. D **9**, 539 (1999).
[62] T.P. Martin, Phys. Rep. **273**, 199 (1996).
[63] A. Mackay, Acta Crystallogr. **15**, 916 (1962).